A peer-reviewed version of this preprint was published in PeerJ on 17 January 2017.

View the peer-reviewed version (peerj.com/articles/2810), which is the preferred citable publication unless you specifically need to cite this preprint.

Lugnani F, Macchioro M, Rubinsky B. 2017. Cryoelectrolysis—electrolytic processes in a frozen physiological saline medium. PeerJ 5:e2810 https://doi.org/10.7717/peerj.2810

Cryoelectrolysis - electrolytic processes in a frozen physiological saline medium

Franco Lugnani [1], **Matteo Macchioro** [2], **Boris Rubinsky** Corresp. [3]

[1] Clinica Santa Elena, Malaga, Spain

[2] Hippocrates D.O.O, Divaca, Slovenia

[3] Department of Bioengineering and Department of Mechanical Engineering, University of California, Berkeley, Berkley, California, United States

Corresponding Author: Boris Rubinsky
Email address: rubinsky@berkeley.edu

Background: Cryoelectrolysis is a new minimally invasive tissue ablation surgical technique that combines the processes of electrolysis and solid/liquid phase transformation (freezing).

Method: Performing a typical cryoelectrolytic ablation protocol in a tissue simulant made of physiological saline gel with a pH dye, we observed several new physical and electrochemical phenomena of relevance to tissue ablation.

Results: We found that electrolysis can occur simultaneously with phase transformation, at high subzero freezing temperatures, above the eutectic temperature of the frozen salt solution. Another interesting finding is that electro-osmotic flows affect the process of cryoelectrolysis at the anode and cathode, in different ways.

Discussion: The observations are consistent with a mechanism involving ionic movement through the concentrated saline solution channels between ice crystals, at subfreezing temperatures above the eutectic. The findings in this paper may become the scientific basis for designing future cryoelectrolytic ablation surgery protocols.

Cryoelectrolysis - electrolytic processes in a frozen physiological saline medium.

Franco Lugnani[1], Matteo Macchioro[2,] Boris Rubinsky[3]

[1]Clinica Santa Elena. Malaga, Spain
[2]Hippocrates D.O.O. Divaĉa, Slovenia
[3]Department of Bioengineering and Department of Mechanical Engineering. University of California Berkeley. Berkeley, CA 94720 USA

Corresponding author:
Boris Rubinsky[3]

Email address: brubinsky@gmail.com

Abstract:
Background: Cryoelectrolysis is a new minimally invasive tissue ablation surgical technique that combines the processes of electrolysis and solid/liquid phase transformation (freezing).
Method: Performing a typical cryoelectrolytic ablation protocol in a tissue simulant made of physiological saline gel with a pH dye, we observed several new physical and electrochemical phenomena of relevance to tissue ablation.
Results: We found that electrolysis can occur simultaneously with phase transformation, at high subzero freezing temperatures, above the eutectic temperature of the frozen salt solution. Another interesting finding is that electro-osmotic flows affect the process of cryoelectrolysis at the anode and cathode, in different ways.
Discussion: The observations are consistent with a mechanism involving ionic movement through the concentrated saline solution channels between ice crystals, at subfreezing temperatures above the eutectic. The findings in this paper may become the scientific basis for designing future cryoelectrolytic ablation surgery protocols.

Introduction.

Minimally invasive and non-invasive surgery have emerged as an important branch of surgery. Cryoelectrolysis is a new minimally invasive tissue ablation surgical technique, that employs freezing and electrolysis, delivered essentially simultaneously, to ablate undesirable tissues. Cryoelectrolysis was developed to overcome drawbacks of the minimally invasive surgery techniques of cryosurgery and of electrolytic ablation, when used separately, while taking advantage of certain valuable attributes of these techniques. While recent studies on animal tissue have demonstrated the advantages of combined cryoelectrolytic ablation over cryosurgery ablation and electrolytic ablation, each used separately, (Lugnani, Zanconati et al. 2015), the fundamental physics of the cryoelectrolytic process was not studied before. This is the first study on the physical and electrochemical processes that occur during cryoelectrolysis.

Cryosurgery is the ablation of undesirable tissues by freezing (Rubinsky 2000). The procedure employs a cryogenic fluid internally cooled cryosurgical probe, inserted in the undesirable tissue. The freezing propagates from the cryoprobe surface outward to freeze and, hopefully, thereby ablate the entire undesirable tissue. An important finding in cryosurgery is that the extent of freezing can be monitored in real time, by essentially every medical imaging techniques (Gilbert, Onik et al. 1984, Onik, Cooper et al. 1984, Rubinsky, Gilbert et al. 1993). This facilitates real time control over the extent of freezing. However, it was also found that cells can survive freezing at high subzero freezing temperatures. Therefore, cells can survive on the outer rim of the frozen lesion or around blood vessels. Thus, the extent of freezing seen on medical imaging does not correspond to the extent of cell death. Motivated by the desire to ablate all the cells in the frozen lesion, "combinatorial" cryosurgery is of current interest to researchers in the field (Baust, Bischof et al. 2015). Combinatorial cryosurgery research deals with attempts to enhance frozen cell ablation through additive chemical mechanisms (Baust, Hollister et al. 1997, Koushafar, Pham et al. 1997, Clarke, Baust et al. 2001, Mir and Rubinsky 2002). Cryoelectrolysis is a new combinatorial surgical technique whose goal is to ablate cells surviving freezing in the high subzero freezing range with products of electrolysis. It draws from the technology of electrolytic ablation.

Electrolytic ablation, also known as Electro-Chemical Therapy (EChT), is a tissue ablation technique that employs products of electrolysis for cell ablation (Nilsson, von Euler et al. 2000). In EChT a direct electric current is delivered to the treatment field through electrodes that are in contact with the tissue. New chemical species are generated at the interface of the electrodes and tissue as a result of the electric potential driven transfer between electrons and ions or atoms in the tissue. The various chemical species produced near the electrodes diffuse away from the electrodes into tissue, in a process driven by differences in electrochemical potential. Tissue ablation is caused by two factors: the cytotoxic environment developing due to local changes in pH, as well as the presence of some of the new chemical species formed during electrolysis. Electrolytic ablation requires very low direct currents (tens to hundreds of mA) and very low voltages (single to low tens of Volts) (Nilsson, von Euler et al. 2000). This is advantageous, because it makes the technology extremely simple and safe. However, the procedure is long, from tens of minutes to hours. The length is related to the slow diffusion of electrochemically

produced species in tissue and the concentration dependent rate of cell death inducing electrochemical reactions. A clinical study on tissue ablation with electrolysis states that— "Currently, a limitation of the technique is that it is time consuming" (Fosh, Finch et al. 2002, Fosh, Finch et al. 2003).

We developed the concept of cryoelectrolysis from the known fundamental observation that freezing of tissue increases the concentration of solutes around cells by removing the water from the solution in the form of ice (Rubinsky and Pegg 1988). Freezing also causes cell membrane lipid phase transition, disrupts the cell membrane lipid bilayer and causes it to become permeabilized (Mir and Rubinsky 2002). It occurred to us that the effects of freezing on the cell membrane permeabilization and on increasing the concentration of solutes near the cells, will expose the interior of cells to the products of electrolysis and enhance cell death; thereby also shortening the time in which electrolysis ablates cells. This is the basic principle of cryoelectrolytic ablation; the combination of solid-liquid phase transformation and electrolysis. Experiments in animal tissue have confirmed our hypothesis and have shown that cryoelectrolysis is more effective at cell ablation than either cryosurgery or electrolytic ablation, alone (Lugnani, Zanconati et al. 2015). This study was designed to yield an understanding of the physical and electrochemical processes which occur during cryoelectrolysis, in particular, how solid/liquid phase transformation and electrolysis occur when delivered simultaneously. Such a study was not done before and the understanding is essential for developing optimal cryoelectrolysis medical treatment protocols.

Materials and Methods

A physiological saline based agar was used to simulate tissue. One liter of water was mixed with 9 grams NaCl and 7 grams of agarose (UltraPure Agarose, Invitrogen). The solution was stirred and heated for 10 minutes and then removed from heat. Two pH indicator dyes were added after five minutes of cooling. For analysis of electrolysis near the anode, methyl red (Sigma-Aldrich®, St. Louis, MO, USA), 1 mL per 100 mL agar solution, was used. For analysis of electrolysis near the cathode we used Phenolphthalein Solution 0.5 wt. % in Ethanol (Sigma-Aldrich) at a concentration of 5 ml per liter agar (or 1 ml per 100 ml agar solution) solution. The agar was cast in a 20 cm diameter cylindrical glass vessel whose radial walls were coated with a 200 μm thick copper foil. The height of the gel cast is 4 cm.

The top two panels in Figure 1, show photographs of the experimental setup. For the cryoelectrolysis experiment we used a Endocare® R2,4 cryoprobe with a diameter of 2.4 mm connected to an Endocare® single port control console device regulating flow duration and monitoring feed-back temperatures (Endocare Inc. Austin, TX, USA). The probe is supplied by a pressurized Argon gas container through the control console, at a constant pressure of 3000 psi. The cooling of the Endocare® stainless steel cryoprobe is through a Joule-Thomson internal valve. The cooling process is typical to all Endocare® cryoprobes of this type. The probe temperature reaches – 180 °C, at a rate of cooling governed in part by the thermal environment in which the probe is inserted. A 30 μm foil of gold was wrapped several times around the cryoprobe, to minimize the participation of the electrode metal in the process of electrolysis. The

metal body of the probe was connected to a DC power supply (Agilent E3631A, Santa Clara CA, USA). In a typical experiment the cryoelectrolysis probe was inserted vertical into the center of the gel. The electrical circuit consists of the power supply, the cryoelectrolysis probe electrode in the center of the gel, the gel and the copper electrode around the gel vessel. The gel was infused with methyl red when the cryoelectrolysis probe served as the anode and with phenolphthalein when the probe served as a cathode. A 1mm T type thermocouple (Endocare®) was inserted to the vicinity of the cryoprobe at a distance of less than 5 mm from the outer surface of the probe, as shown in Figure 1, and the temperature was recorded continuously, throughout the experiment. It should be emphasized that this is not the temperature of the probes. A camera was focused on the experimental setup to continuously record the position of the change of phase interface, the position of the pH front, the voltage, current and time.

Insert Figure 1 here

The following experimental procedure was employed in all the experiments. The electrical circuit, comprised of the cryoelectrolysis probe, the gel and the copper vessel walls, was connected to the power supply first. It remained connected throughout the experiment, during freezing and thawing. The flow of cryogen began one minute after the circuit was connected to the power supply. Constant pressure of 3000 psi was used to generate the Argon gas flow in a manner typical to clinical cryosurgical treatment with the probe we used. The flow of cryogen was delivered for ten minutes after which the flow was stopped and the frozen lesion was left to thaw, in situ. The electrical circuit remained connected to the power supply for additional 15 minutes after the flow of the cryogen was stopped. The current was set to various values of 400 mA, 200 mA and 50 mA, in different experiments, and the voltage was allowed to change to provide the desired current. However, the saturation voltage of the power supply is 25V and the system cannot provide a higher voltage. Therefore, when changes in resistance demanded a voltage higher than 25V, the current dropped. Following 30 experiments to identify the parameters that are most likely to provide physical and electrochemical insight into the cryoelectrolysis process, we identified the protocol listed above as optimal for generating a good insight into the fundamental aspects of cryoelectrolysis. We followed with 18 systematic cryoelectrolysis experiments with the parameters listed above. This paper reports the results from the last series of experiments.

Results and discussion

Figure 1, also presents a compilation of photographs that illustrate several important observations, typical to all the experiments performed in this study. Panels 1C, and 1D, are images of the progression of the pH front during a process in which there was only electrolysis, without cooling. The cryoelectrolysis probe served as the anode and delivered 400 mA. Panel 1C, shows the radially symmetric pH front around the anode. The process of electrolysis was continued for several minutes and panel 1D shows the pH front at a later time. Obviously the pH front has advanced, while remaining radially symmetric. The white arrow points to an observation of importance to cryoelectrolysis. Diffusion and iontophoresis driven electro-

osmosis, are the physical mechanisms that cause the propagation of the pH front from the electrode outward. The electro-osmotic flow is an important aspect of electrolytic ablation in tissue (Lugnani, Zanconati et al. 2015, Phillips, Raju et al. 2015, Phillips, Rubinsky et al. 2015, Rubinsky, Guenther et al. 2015, Stehling, Guenther et al. 2016). The flow is from the anode to the cathode. The white arrow points to a dark gap that has formed between the electrode and the gel. (Inserts in Fig 1 are magnified views of the region near the electrode) The gap was caused by the electro-osmotic driven flow of solution, away from the anode, towards the cathode. The later panels in this figure will illustrate the significance of this electro-osmotic flow to cryoelectrolysis.

Panels 1E, and 1F, are images of the progression of the pH front and of the ice front during a typical cryoelectrolytic protocol of the type described in the materials and methods section. The cryoelectrolysis probe served as anode and delivered 400 mA. Panel 1E shows the appearance of the frozen lesion at the end of the cooling stage of the protocol. The dashed arrow point to the edge of the frozen lesion. Panel 1F is a photograph from the same experiment taken several minutes after the cooling was stopped, while the power supply continued to deliver current to the electrical circuit. Two interesting observations emerge. While the extent of the frozen lesion in panel 1F has not changed from that in panel 1E; the pH front has advanced beyond the frozen lesion. This demonstrates that the process of electrolysis can occur through ice. The mechanism will be discussed in the context of Figures 2 and 3. The white arrow shows that the electro-osmotic flow generated gap formed between the electrode and the gel during conventional electrolysis, also occurs during cryoelectrolysis. This further strengthens the evidence that electrolysis occurs through a frozen region.

Panels 1G, and 1H, are images of the progression of the pH front and of the ice front during a typical cryoelectrolytic protocol of the type described in the materials and methods section. The cryoelectrolysis probe served as the cathode and delivered 50 mA. Obviously, the appearance of the treated areas in panels 1G and 1H is completely different from that in panels 1E and 1F. Panel 1G is from an earlier stage of the cryoelectrolysis protocol, during which, both electrical current and cryogen cooling, were delivered by the cryoelectrolysis probe, simultaneously. It is important to observe that both, a pH front and an ice front have formed and they propagate in an asymmetric way. The lack of symmetry is evident in comparison with panel 1E. The difference is caused by the direction of the electro-osmotic flow, which in this case, is towards the cryoelectrolysis cathode probe. This generates a high flow rate of solution, at the cryoelectrolysis cathode probe interface. We have observed a flow of water gushing out at the interface between the cryoelectrolysis probe and the gel, regardless of the current magnitude used and in all the cryoelectrolysis cathode probe study repeats. The water also contains a mixture of gas (hydrogen from the reduction reaction near the cathode). Evidence of the process can be seen from the red dots spread over the right hand side of the gel (dotted arrow in panel 1G). The red dots are caused by the splashed droplets of high pH fluid. The electro-osmotic pressure has caused various random and detrimental effects, when the cryoelectrolysis probe is the cathode. For higher currents, of 200 mA and 400 mA, the electro-osmotic pressure driven flow has caused fractures and cracks in the gel. For the lower currents of 50 mA it produced the lack of symmetry seen in panels 1G and 1G. The electro-osmotic pressure caused events, occur at random and the cracks formation is not predictable.

Panel 1G was taken during the last stage of the experiment; a stage in the typical cryoelectrolysis protocol in which the cooling was stopped and only electrolysis occurs. This is at a similar stage in the protocol to that in which panel 1F photograph was taken. Here, we observe that the pH front has propagated irregularly both within and beyond the frozen lesion. The propagation of the pH front occurred while the frozen lesion still exists. This demonstrates that the process of electrolysis can occur through a frozen domain when the cryoelectrolysis probe is either anode or cathode. The lack of symmetry in the appearance of the pH front in panel 1F can be, probably, attributed to cracks that form in the gel because of the electro-osmotic pressure. These cracks favor certain directions of propagation of the electrolytic products flow. The magnified insert of the region near the cryoelectrolysis cathode probe provides further evidence on the effect of the electro-osmotic flow. The dark gap between the cryoelectrolysis anode probe and the gel in panels 1D and 1F does not form when the cryoelectrolysis probe is the cathode. In fact, the white arrows point to a bulging volume of ice formed in the vicinity of the cryoelectrolysis probe. The insert also shows a crack in the gel, filed with ice. In summary, this part of the study reveals two important physical phenomena related to cryoelectrolysis: a) electrolysis can occur through a frozen milieu at both, the anode and the cathode, b) electro-osmotic flows play an important part in the physical events that occur during cryoelectrolysis. Because of electro-osmotic flows the outcome of the procedure, is different between a cryoelectrolysis cathode probe and a cryoelectrolysis anode probe.

Figures 2 and 3 were chosen to illustrate the events that occur during typical processes of cryoelectrolysis. The cryoelectrolysis probe was the anode and the constant set current, 200 mA. Figure 2 is a sequence of images showing the pH front and the ice front at different instances in time during the cryoelectrolysis protocol. Figure 3 is from the same experiment. It displays, from top to bottom: the diameters of the pH front and of the ice; the measured current, the measured voltage, the calculated resistance and the temperature of the thermocouple,

Insert Figure 2

Panel 2A, shows the appearance of the pH front, one minute after the start of the experiment, just prior to the start of the cooling process. The current is 200 mA and the voltage is about 8 V. Panel 2B shows the appearance of the ice front and of the pH front one minute after the start of freezing and two minutes after the start of the experiment. It is evident from comparison with panel 2A that during this one minute of freezing, the ice front and the pH front have both advanced. Figure 3 shows that in this period of time, as the temperature near the probe drops below freezing and the change of phase advances, the voltages increases and reaches the 25 V saturation level after which the current begins to decrease. Obviously this is caused by an increase in resistance in the freezing domain. Nevertheless, both panel 2B and the data in Figure 3 show that electrolysis occurs in this early, high subzero temperature stage of the freezing process.

Panels 2C, 2D and Figure 3 show that after one minute of freezing, the pH front stops advancing (no electrolysis) while the ice front propagates further. Figure 3 shows that in this period the

temperature drops further, the electrical resistance of the frozen lesion increases to high values and the flow of electrical current stops. This effect of freezing is expected, as ice has a negligible electrical conductivity.

Interesting physical events, never reported before, are observed after cooling was stopped, i.e. 11 minutes after the start of the experiment. The temperature measurements hold the explanation for the mechanism. Figure 3 shows that the temperature measured by the thermocouple begins to raise as soon as the cooling stops. However, the temperature remains close and below the phase transformation temperature for most of the remainder of the cryoelectrolysis protocol. This phenomenon was observed and reported in the past, (Rubinsky and Cravalho 1979). As explained in (Rubinsky and Cravalho 1979), the phenomenon is related to the fact that the change in enthalpy during phase transition of ice into water is very large relative to the change in enthalpy due to change in temperature in ice. Briefly, during melting, heat is extracted from the frozen domain, through the change of phase interface, by the environment surrounding the interface. The temperature of the interface is fixed by equilibrium thermodynamics of a two phase system at constant pressure. As long as there is an ice and water mixture in a domain, the temperature of that domain cannot exceed the thermodynamic phase transition temperature of the solution. The phase transformation process (melting) occurs only on the change of phase interface, which propagates very slowly, because the large change in enthalpy involved. Since the enthalpy associated with changes of temperature in the frozen domain are very small relative to the change in enthalpy by phase transformation, the temperature of the frozen region becomes elevated and reaches the phase transition temperature fast, throughout the frozen region; while the region is still frozen (Rubinsky and Cravalho 1979). Consequently, while the extent of the frozen regions remains essentially unchanged at the end of cooling (panels 2E to 2G) the temperature of the frozen region raises to become close and below the change of phase temperature. The temperature measurements in Figure 3 validate this explanation. The increase in the temperature of the frozen region has several effects. Figure 3 shows that there is a gradual increase in current and a decrease in resistance. Consequently, there is a process of electrolysis, and the pH front expands beyond the margin of the frozen region, while the region is still frozen (panels 2F to 2I).

Insert Figure 3

The mechanism responsible for electrolysis in a high subzero frozen media is associated with the process of freezing in solutions and tissues. Ice has a tight crystallographic structure and cannot contain any solutes. Constitutional supercooling dictates that during freezing of a solution, finger like ice crystals form and the salt is rejected along the ice crystals (Rubinsky 1983). High concentration salt solutions form along the ice crystals. This phenomenon occurs during freezing of any aqueous medium, in solutions (Ishiguro and Rubinsky 1994), gels (Preciado, Shandakumaran et al. 2003) and tissues (Rubinsky and Pegg 1988). While ice electrical conductivity is essentially zero, electrical currents can flow through these high concentration brine channels until the temperature reaches the eutectic – 21.1 °C. Figure 3 shows that indeed current flows through the high subzero temperature region of frozen gel. Unavoidable, flow of ionic current is associated with electrolysis and this is why the pH front advances while the tissue

is still frozen. The flow of current through the brine channels most likely elevated the local temperature of these channels and may cause local melting and expansion or collapse of the brine channels. It is possible that this phenomenon is responsible for the jumps in voltage measured occasionally after the freezing stops (see Fig. 3).

Conclusion

The combined effect of freezing and electrolysis was studied in a tissue simulant made of a physiological solution of agar with pH dyes. To the best of our knowledge, this is the first time that electrolysis through ice was observed and reported. This finding is valuable for designing cryoelectrolysis protocols. It demonstrates that the processes of freezing and of electrolysis can be done effectively simultaneously. It appears that the most effective period for delivering electrolytic currents is immediately after cooling has stopped.

Acknowledgement: We are grateful to Dr. Liel Rubinsky who did the first work on cryoelectrolysis and whose work planted the seeds for this paper and to Mr. Paul Mikus for useful advice.

References:

Baust, J. G., J. C. Bischof, S. Jiang-Hughes, T. J. Polascik, D. B. Rukstalis, A. A. Gage and J. M. Baust (2015). "Re-purposing cryoablation: a combinatorial 'therapy' for the destruction of tissue." Prostate Cancer and Prostatic Diseases **18**(2): 87-95.

Baust, J. G., W. Hollister, A. Mathews and R. Van Buskirk (1997). "Gene-regulated cell death follows cryosurgery." Cryobiology **35**(4): 322-322.

Clarke, D. M., J. M. Baust, R. G. Van Buskirk and J. G. Baust (2001). "Chemo-cryo combination therapy: An adjunctive model for the treatment of prostate cancer." Cryobiology **42**(4): 274-285.

Fosh, B. G., J. G. Finch, A. A. Anthony, M. M. Lea, S. K. Wong, C. L. Black and G. J. Maddern (2003). "Use of electrolysis for the treatment of non-resectable hepatocellular carcinoma." Anz Journal of Surgery **73**(12): 1068-1070.

Fosh, B. G., J. G. Finch, M. Lea, C. Black, S. Wong, S. Wemyss-Holden and G. J. Maddern (2002). "Use of electrolysis as an adjunct to liver resection." British Journal of Surgery **89**(8): 999-1002.

Gilbert, J. C., G. M. Onik, W. K. Hoddick and B. Rubinsky (1984). "The use of ultrasound imaging for monitoring cryosurgery." IEEE Transactions on Biomedical Engineering **31**(8): 565-565.

Ishiguro, H. and B. Rubinsky (1994). "Mechanical Interaction between ice crystals and red blood cells during directional solidification." Cryobiology **31**(5): 483-500.

Koushafar, H., L. Pham, C. Lee and B. Rubinsky (1997). "Chemical adjuvant cryosurgery with antifreeze proteins." Journal of Surgical Oncology **66**(2): 114-121.

Lugnani, F., F. Zanconati, T. Marcuzzo, C. Bottin, P. Mikus, E. Guenther, N. Klein, L. Rubinsky, M. K. Stehling and B. Rubinsky (2015). "A Vivens Ex Vivo Study on the Synergistic Effect of Electrolysis and Freezing on the Cell Nucleus." Plos One **10**(12).

Mir, L. M. and B. Rubinsky (2002). "Treatment of cancer with cryochemotherapy." British Journal of Cancer **86**(10): 1658-1660.

Nilsson, E., H. von Euler, J. Berendson, A. Thorne, P. Wersall, I. Naslund, A. S. Lagerstedt, K. Narfstrom and J. M. Olsson (2000). "Electrochemical treatment of tumours." Bioelectrochemistry **51**(1): 1-11.

Onik, G., C. Cooper, H. I. Goldberg, A. A. Moss, B. Rubinsky and M. Christianson (1984). "Ultrasonic characteristics of frozen liver." Cryobiology **21**(3): 321-328.

Phillips, M., N. Raju, L. Rubinsky and B. Rubinsky (2015). "Modulating electrolytic tissue ablation with reversible electroporation pulses." Technology **3**(1): 45-53.

Phillips, M., L. Rubinsky, A. Meir, N. Raju and B. Rubinsky (2015). "Combining Electrolysis and Electroporation for Tissue Ablation." Technology in Cancer Research & Treatment **14**(4): 395-410.

Preciado, J. A., P. Shandakumaran, S. Cohen and B. Rubinsky (2003). Utilization of directional freezing for the construction of tissue engineering scaffolds. ASME 2003 International Mechanical Engineering Congress and Exposition, Washington DC.

Rubinsky, B. (1983). "Solidification processes in saline solutions. ." Journal of Crystal Growth **62**(3): 513-522.

Rubinsky, B. (2000). "Cryosurgery." Annual Review of Biomedical Engineering **2**: 157-187.

Rubinsky, B. and E. G. Cravalho (1979). "Analysis for the temperature Distribution During the Thawing of a Frozen Biological Organ." A.I.Ch.E. Symposium Series, **75**: 81-88.

355 Rubinsky, B., J. C. Gilbert, G. M. Onik, M. S. Roos, S. T. S. Wong and K. M. Brennan (1993).
356 "Monitoring cryosurgery in the brain and in the protstate with proton NMR. ." Cryobiology
357 **30**(2): 191-199.
358 Rubinsky, B. and D. E. Pegg (1988). "A mathematical model for the freezing process in biological
359 tissue. ." Proceedings of the Royal Society of London Series B-Biological Sciences **234**(1276):
360 343-349.
361 Rubinsky, L., E. Guenther, P. Mikus, M. Stehling, K., and B. Rubinsky (2015). "Electrolytic Effect
362 During Tissue Ablation by Electroporation." Technology in cancer Research and Treatement.
363 Stehling, K., M.,, E. Guenther, P. Mikus, N. Klein, L. Rubinsky and B. Rubinsky (2016). "Synergistic
364 combination of electrolysis and electroporation for tissue ablation." PLoS ONE **11(2)**: e0148317.

List of Figures:

Figure 1: Experimental layout and illustration of typical cryoelectrolysis process. A) Photograph of experimental system: a – electrode on container surface, b – cryoelectrolysis probe, c – DC power supply, d – thermocouple, e – camera, f – cryosurgery probe pressure monitor; B) close-up of the gel and electrodes; Photographs of the pH front and freezing front in different experiments: C) electrolysis only, 400 mA current, D) pH front at a later time, E) cryoelectrolysis with cryoelectrolysis probe at the anode, 400 mA, F) pH front and ice front at a later time, cryoelectrolysis probe at the anode with 400mA current, G) cryoelectrolysis with cryoelectrolysis probe at the cathode, 50 mA, H) pH front and ice front at a later time, cryoelectrolysis probe at the cathode, 50mA current. Top photo earlier time. Black arrow – pH front, black dashed arrow - ice front, white arrow – interesting feature near the cryoelectrolysis probe. In the same panel, both photographs are to the same scale.

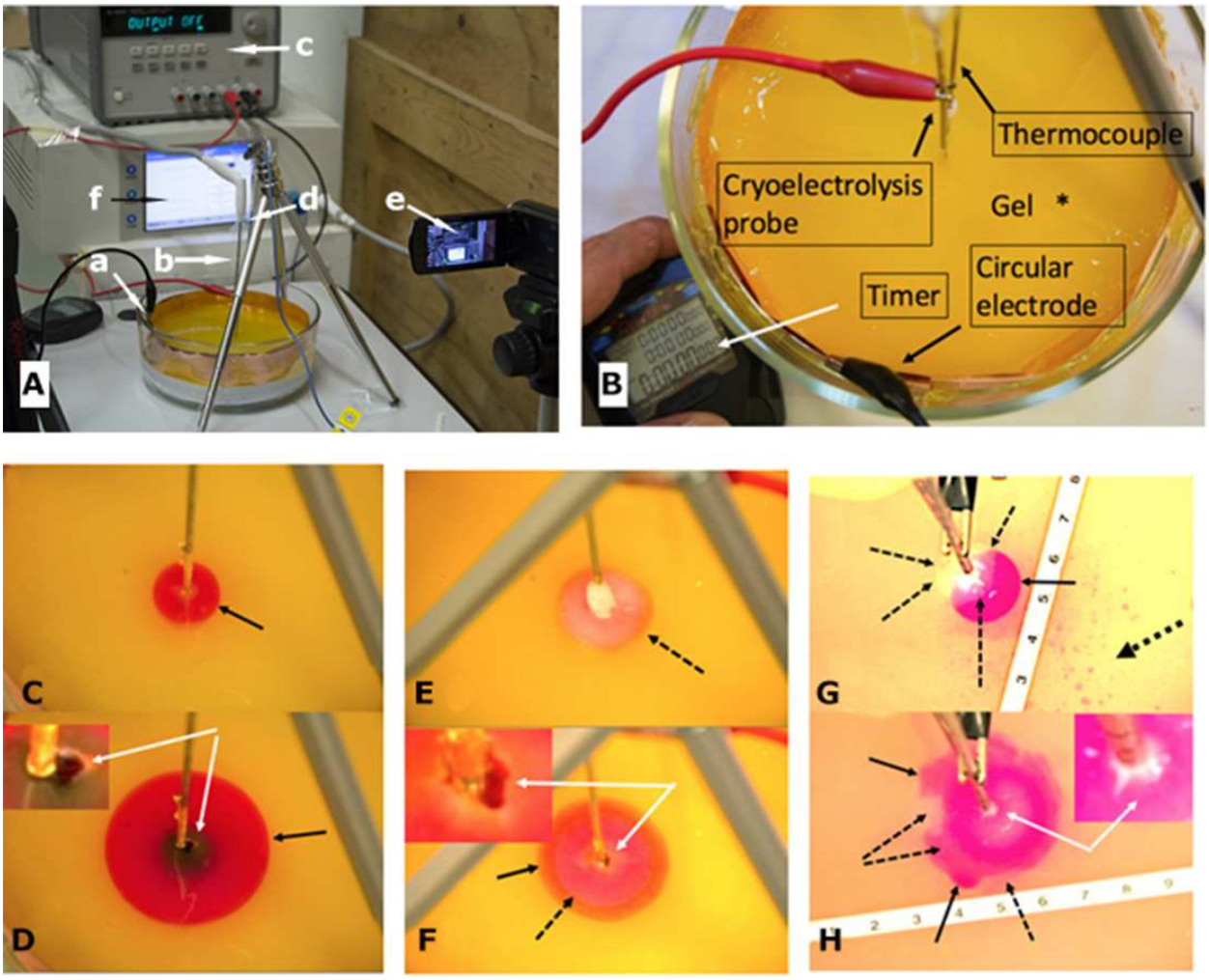

Figure 2: progression of a pH front and a cryoelectrolysis front during a typical cryoelectrolysis protocol. Results shown as a function of time after the start of the experiment (in minutes); a) 1, b) 2, c) 3.5, d) 11, e) 12.5, f) 16, g) 18.5, h) 21, i) 26. All the figures are at the same scale (cm scale shown). The margin of the pH front is marked with a dark arrow and of the ice front with a dotted dark arrow. A feature of interest near the cryoelectrolysis probe marked with a white arrow.

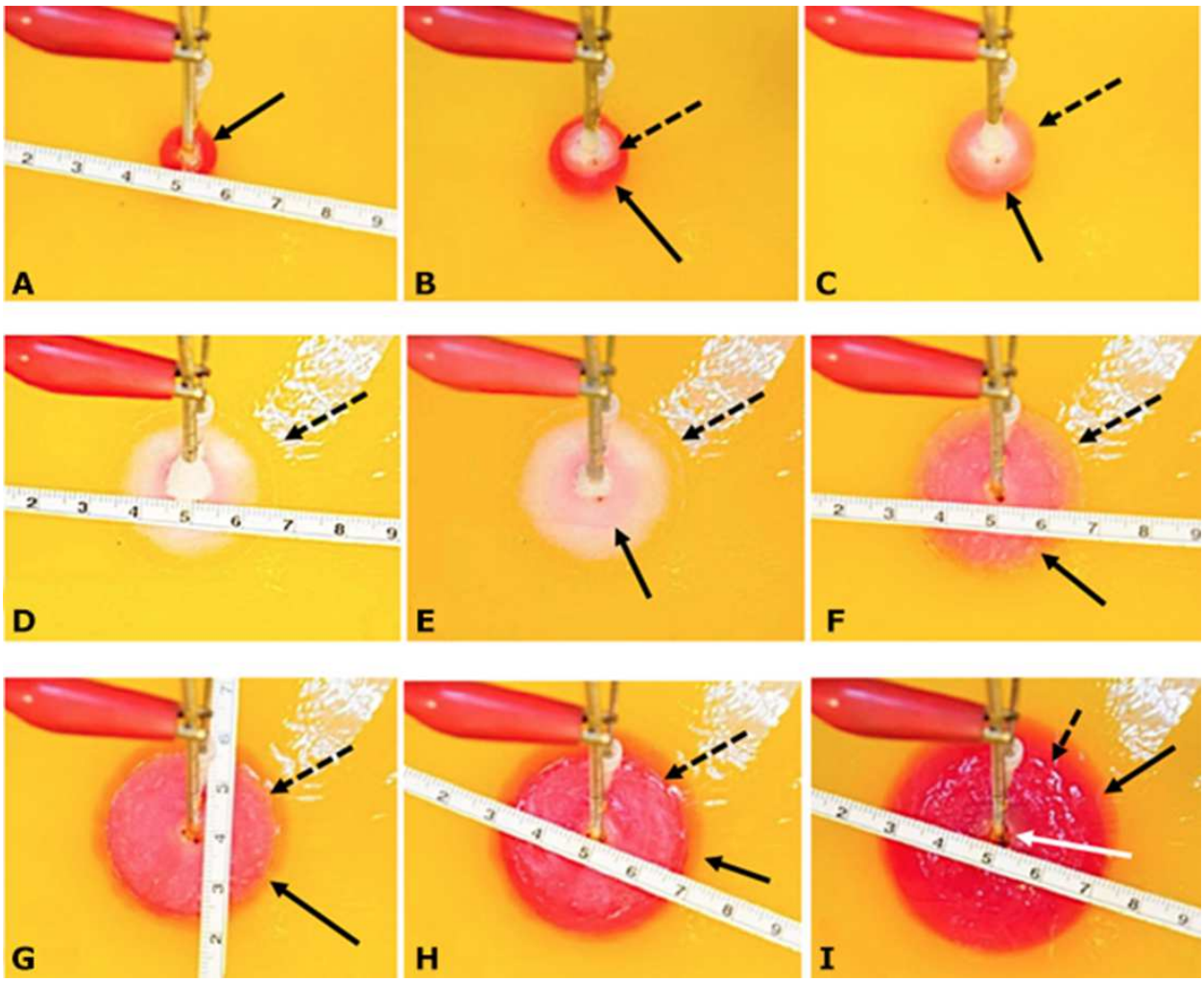

Figure 3: data from an experiment in which the cryoelectrolysis probe served as the anode and the fixed current was 200 mA. The diameter of the ice front (dashed line) and of the pH front (solid line); current; voltage; overall resistance; temperature, as a function of time in minutes.